Notes

Effect of Iodine-Catalyzed Isomerization on the Optical Properties of Poly[(1,3-phenylenevinylene)-*alt*-(2,5-hexyloxy-1,4-phenylenevinylene)]s

Liang Liao and Yi Pang*

Department of Chemistry & Center for High Performance Polymers and Composites, Clark Atlanta University, Atlanta, Georgia 30314

Liming Ding and Frank E. Karasz

Department of Polymer Science and Engineering, University of Massachusetts, Amherst, Massachusetts 01003

Received December 10, 2001
Revised Manuscript Received May 20, 2002

Introduction

Since the discovery of polymeric light-emitting diodes (LEDs)[1] in 1990, π-conjugated polymers have attracted increasing attention over the past decade[2] because of their potential applications in display technologies. The unique combination of their structural, mechanical, photonic, and electronic properties also renders them attractive candidates for use as plastic lasers,[3] chemical sensors,[4] and in other fields.[5] Recent studies[6] have shown that poly[(*m*-phenylenevinylene)-*alt*-(*p*-phenylenevinylene)] derivatives **3** (PmPVpPV) are green-emitting with high photoluminescence (PL) efficiency. The polymers are generally synthesized via using the Wittig condensation reaction (Scheme 1). The majority[6a] of the vinylene linkages in the polymers **3** are in the *cis*-configuration. Although polymer **4** with *trans*-vinylene linkages can be obtained by refluxing the toluene solution of **3** in the presence of a catalytic amount of iodine, the polymer thus obtained may be contaminated by iodine, which is known to decrease the PL quantum yield[7] via the so-called "heavy-atom" effect. In the iodine-catalyzed isomerization, the reaction may proceed via a thermally induced iodine radical process as proposed in the conjugated olefin system.[8] Although only a catalytic amount of iodine (∼0.2−0.3 wt %) is used in the reaction, some iodine atom may be chemically bonded to the product to generate some structural defects along the polymer backbone, which may adversely affect the optical properties of the polymers.

The iodine-free PmPVpPV with a high content[9] of *trans*-vinylene linkages (**6a**) has been synthesized via the Wittig−Horner reaction. The solution PL efficiency of **6a** ($\phi_{fl} \approx 0.64$ in THF) is measured to be the same as that of **4a**, while the PL emission λ_{max} of the former is slightly red-shifted ($\Delta\lambda_{max} = 1-2$ nm). To further evaluate the impact of the iodine treatment to the optical properties of PmPVpPV samples, especially in the film state, we have made a comprehensive comparison between polymers **4** and **6**, which have similar content of *trans*-vinylene linkage. Since the iodine-catalyzed isomerization remains to be a common method used in synthesizing poly(phenylenevinylene) (PPV) materials,[10] understanding the overall impact of the iodine treatment to the π-conjugated polymers, therefore, is desirable for the future development of luminescent polymers.

Scheme 1

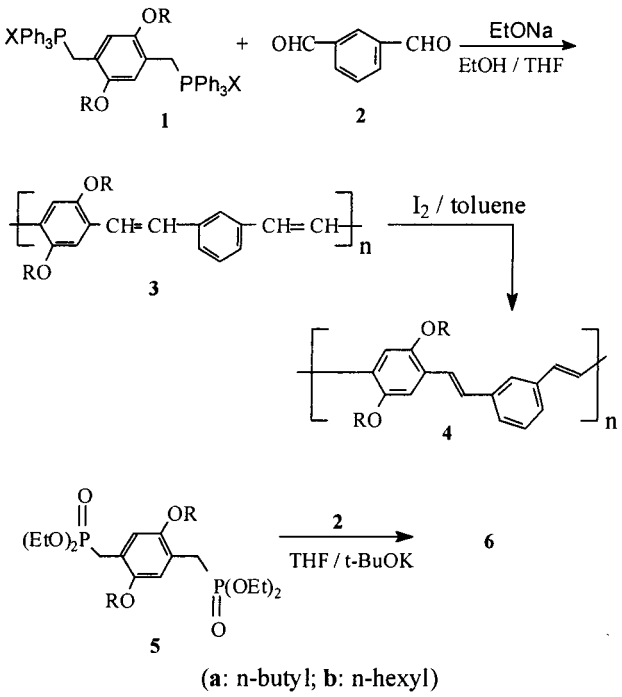

Results and Discussion

The iodine-catalyzed isomerization of *cis*-1,2-diarylethene (**7**) might proceed similarly as proposed for the isomerization of conjugated dienes.[8] As shown in Scheme 2, addition of an iodine radical to **7**, followed by rotation of the carbon−carbon single bond, produced the radical **8**. Regeneration of the iodine radical from **8** would lead to the desired *trans*-1,2-diarylethene (**9**). Hydrogen abstraction from **8** or recombination of **8** with an iodine radical produced the respective iodine-contaminated structures **10** or **11**. Elemental analysis of **4b** showed that the sample contained ∼0.26% iodine elements, indicating that about 1 per 241 phenylenevinylene units[11] might contain an iodine atom introduced during the isomerization process. The average number of phenylenevinylene units for polymer **4b** is estimated to be only 71, by using the number-average molecular weight (Table 1). This result suggests that only a small fraction (less than 30%) of polymer chains is contaminated by iodine. Both infrared and NMR (^{1}H and ^{13}C) spectra detected no difference between polymers **4** and **6**, supporting the assumption that the iodine contamination in the former would be very low.

10.1021/ma012144j CCC: $22.00
Published on Web 06/18/2002

Scheme 2

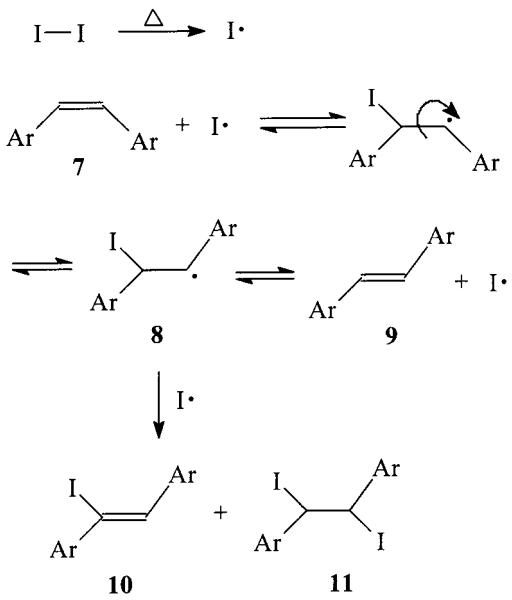

Photoabsorption and Photoluminescence of Solutions. Figure 1 shows the UV−vis spectra of **4b** and **6b** in THF solution at room temperature, exhibiting two absorption bands (λ_{max} = 328 and ∼406 nm). The λ_{max} value of the low-energy absorption band was measured to be 406 and 410 nm for polymers **4b** and **6b**, respectively. As the temperature was lowered from 25 to −108 °C (still in solution state), both spectra were red-shifted similarly, indicating the adoption of a more planar conformation at the low temperature. In addition, the low-energy absorption band was resolved into two bands at −108 °C (λ_{max} = 415 and 437 nm for **4b** and λ_{max} = 420 and 438 nm for **6b**), due to the reduced rotation and increased solvent viscosity at the low temperature.

Fluorescence spectra of **6b** and **4b** at room temperature (Figure 2) revealed a very similar emission profile with emission λ_{max} at 447 and 475 nm. The solution fluorescence quantum efficiencies ϕ_{fl} (Table 1) for polymers **4** and **6** were comparable. Although both polymers gave more intense emission at 447 nm, their relative emission intensities at 475 nm were different. The possible iodine contamination in **4**, therefore, appeared to have only a small effect on the luminescent property of the molecule, which is in agreement with the fact that the concentration of the iodine-contaminated repeating unit is very low.

As the temperature was lowered to −108 °C, the spectra were also noticeably red-shifted with emission peaks at 454, 491, and 526 nm (corresponding to the wavenumber of 22 026, 20 367, and 19 011 cm^{-1}, respectively). The emission peaks appeared to be about equally spaced with a wavelength separation of ∼35 nm (or a wavenumber separation of ∼1659 cm^{-1}), which is

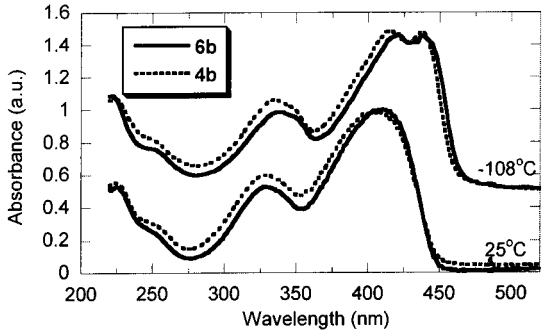

Figure 1. UV−vis spectra of **6b** (solid line) and **4b** (broken line) in THF at 25 and −108 °C. The spectra at different temperature are offset for clarity.

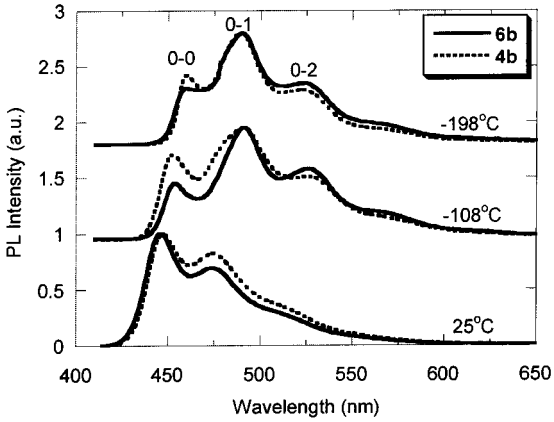

Figure 2. Normalized solution PL spectra of **6b** (solid line) and **4b** (broken line) at 25 and −108 °C in THF and at −198 °C in a solvent mixture (diethyl ether, ethanol, and 2-methylbutane in a ratio of 1:1:1). The spectra at different temperature are offset for clarity.

larger than the difference between the high-energy emission band (at 454 nm) and the low-energy absorption band (at ∼437 nm). On the basis of the theoretical model[12] of an anharmonic oscillator, the emission peaks of 454, 491, and 526 nm in the spectrum of −108 °C were assigned to the 0−0, 0−1, and 0−2 transitions, respectively. Interestingly, the 0−1 band became the most intense emission at −108 °C. When the temperature was lowered to −198 °C (sample was completely frozen), the relative intensity of the 0−1 band was further slightly increased at the expense of the 0−0 band. This change in relative emission intensity was apparently related to the molecular conformation change at the low temperature, which was observed from the bathochromic shifts in both absorption and fluorescence spectra.

Thin Film Optical Properties. Figure 3 showed the absorption spectra of films cast on the quartz surface. The absorption profile of **4b** overlapped very well with that of **6b** at room temperature. As the films were

Table 1. Comparison of Spectroscopic Data for PmPVpPV 4 and 6

polymer	content of *trans*-CH=CH	UV−vis λ_{max} (nm)[a]	fluorescence λ_{max} (nm)[a]	film UV−vis λ_{max} (nm)	film PL λ_{max} (nm)	ϕ_{fl}[b]	M_w (PDI)[c]
4a	91	328, 402	444, 469	335, 411	506, 532	0.65	25 000 (1.4)
6a	88	328, 404	445, 471	336, 412	503, 531	0.64	11 590 (2.1)
4b	95	328, 407	447, 475	336, 422	507	0.60	20 200 (1.4)
6b	96	328, 410	447, 475	337, 422	530	0.63	45 000 (2.0)

[a] The optical data are acquired from the THF solution at room temperature. [b] The fluorescence quantum efficiency values are estimated in THF solution by using the conditions reported previously. [c] M_w and PDI of the polymers are determined by using gel permeation chromatography equipped with on-line refractive index, light-scattering, and viscometer detectors.

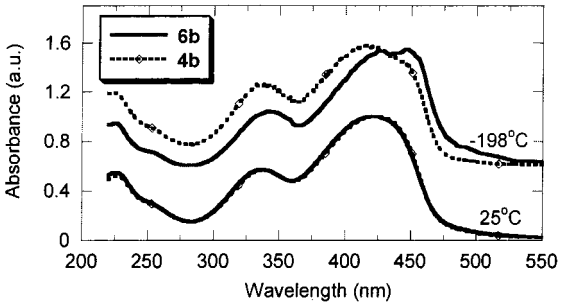

Figure 3. UV−vis spectra of films **6b** (solid line) and **4b** (broken line) on quartz at 25 and −198 °C. The spectra at different temperature are offset for clarity.

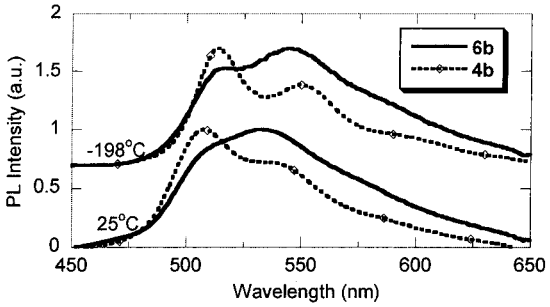

Figure 4. PL spectra of films **6b** (solid line) and **4b** (broken line) on quartz at 25 and −198 °C. The spectra at different temperature are offset for clarity.

immersed in liquid nitrogen (at −198 °C), however, the spectrum of **6b** was noticeably red-shifted (∼8 nm) from that of **4b**. As previously shown from their solution absorption spectra (Figure 1), the chromophores in both **6b** and **4b** had a similar tendency to adopt a more planar molecular conformation at the low temperature. The tendency for the chromophores in the polymers to achieve a more planar conformation was greatly reduced in the film state, as the motion of the polymer chains was restricted. The observed bathochromic shift of the film **6b** from the film **4b** at the low temperature suggested that the chromophore in the former was packed in a slightly different environment than that in the latter. The presence of the small amount of the structural defects present in **4b** could interfere with the molecular packing in the film state, thereby resulting in a difference between the packing environments for the films **4b** and **6b**.

At −198 °C, the broad low-energy absorption band of **6b** appeared to be resolved into two peaks (λ_{max} at 425 and 446 nm), attributing to the further reduced vibration and rotation at the low temperature. The difference ($\Delta\lambda_{max} = 21$ nm) between the two newly resolved peaks in the film **6b** at the low temperature matched very well with that ($\Delta\lambda_{max} = 18$ nm) observed from its solution at −108 °C, indicating that the resolved absorption bands in the film were intrinsic molecular properties of the chromophore in the polymer. In comparison with the film **6b**, the absorption band of **4b** was less resolved at −198 °C, which seemed to be in agreement with the assumption that the chromophore in the latter had a less planar conformation.

Although the absorption spectra of films **4b** and **6b** exhibited nearly the same profile at room temperature, their PL spectra showed a noticeable difference (Figure 4). At −198 °C, the broad emission peak of film **6b** was partially resolved into two bands with λ_{max} at 516 and 544 nm, which matched very closely with the emission peaks of 516 and 549 nm from the film **4b**. The observed similarity in the vibronic structure of films **4b** and **6b** confirmed the presence of the same emission chromophore in both polymers. Polymers **4b** and **6b** exhibited a quite different emission intensity ratio at peaks 516 and 544 nm, indicating the potential influence of the trace structural defects on the luminescent property. In addition, the PL spectra of the polymer at −198 °C were slightly red-shifted (about 7−14 nm) from that at room temperature. This PL spectral red shift is much smaller than that observed from MEH−PPV films (∼32 nm)[13] when the temperature was changed in a similar range (from 12 to −192 °C), partially attributed to the defined conjugation length present in both **4** and **6**.

The corresponding wavenumber for the emission peaks at 516 and 544 nm are 19 380 and 18 382 cm^{-1}. The wavenumber separation between the adjacent vibronic energy levels in the films, therefore, was estimated to be 998 cm^{-1}. The wavenumber separation between the absorption band of the lowest energy at 446 nm (22 422 cm^{-1}, Figure 3) and the emission band of the highest energy at 516 nm (Figure 4) was estimated to be 3042 cm^{-1}, which was slightly more than three times as large as the adjacent viberational energy gap of ∼998 cm^{-1} in the ground state (observed from the emission spectrum). The large separation between the absorption band at 446 nm and the emission band at 516 nm suggested that the emission peaks at 516 and 544 nm from the films could originate from the 0−1 and 0−2 transitions, respectively. The assignment appeared to be in agreement with the observation from the solution PL spectra, where the emission from the 0−1 and 0−2 transition increased greatly at the expense of the 0−0 emission when the molecule was frozen into a rigid environment (Figure 2).

To compare the PL quantum efficiency in the solid state, thin films of **6b** and **4b** were prepared on quartz plates. To minimize the effect of film thickness, the films were spin-cast from their solutions so that their absorbance values at absorption λ_{max} were between 0.09 and 0.1. At room temperature, film **6b** exhibited a constantly higher emission intensity[14] than that of **4b**. The observed larger impact from the trace iodine element in the polymer films, in comparison with their solution PL efficiencies, could be rationalized by considering the interaction between the chemically bound iodine element and polymer chain. In the dilute solution, interaction between the iodine and polymer chain is predominantly limited to intramolecular interaction. In the films, however, the intimate packing of polymer chains permits the trace iodine element to interact both intra- and intermolecularly with the neighboring polymer chains, thereby allowing each iodine atom to exert an influence on more than one molecule.

EL Properties. LED devices were fabricated under the identical experimental conditions to compare the EL properties. The double-layer device ITO/PEDOT/**4b** or **6b** /Ca gave a green emission, although the emission peaks of **4b** (at 513 and 539 nm) was slightly red-shifted from that of **6b** (513 and 523 nm). The EL spectra (Figure 5) of **4b** and **6b** conformed very well with their respective film PL spectra, indicating that both PL and EL originated from the same radiative decay process of the singlet exciton.[16] The turn-on voltage for the device of **6b** (∼3.5 V) was noticeably lower than that for **4b** (∼5 V). In addition, the external quantum efficiency for the device of **6b** (0.16%) was remarkably higher than

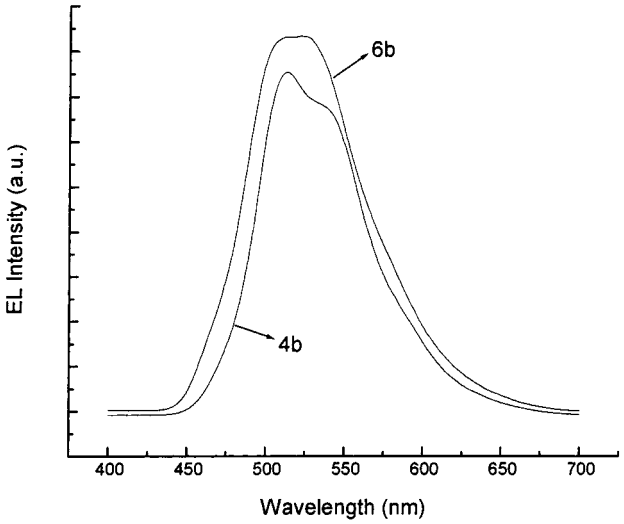

Figure 5. Electroluminescence of polymers **4b** and **6b** with the device configuration ITO/PEDOT/polymer/Ca.

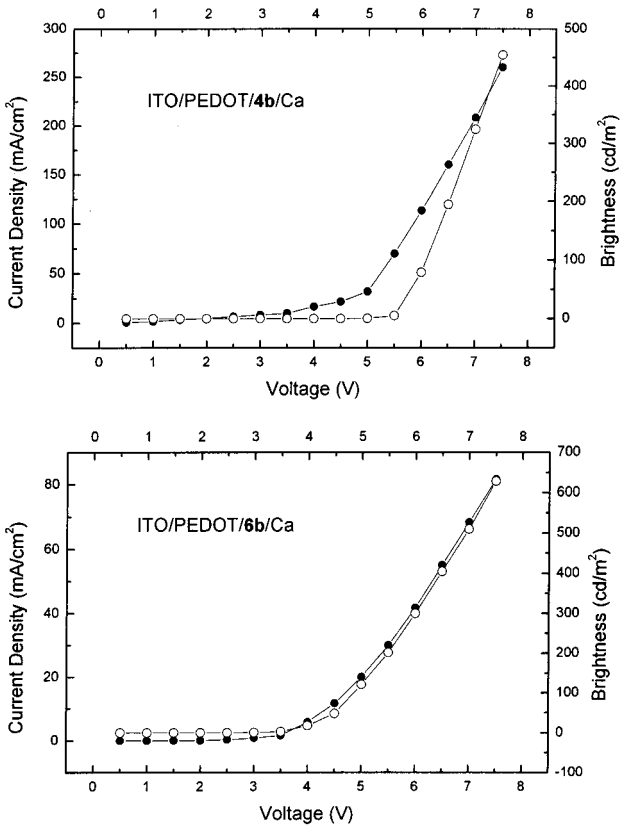

Figure 6. Current density (●)−voltage−brightness (○) relationship for the device ITO/PEDOT/polymer/Ca.

that for **4b** (0.036%). The drastic improvement in the device efficiency is apparently due to the balanced electron/hole injection achieved in the polymer layer **6b** (Figure 6). The lower EL efficiency of **4b** is clearly associated with the presence of trace iodine contaminant, which lowers its PL efficiency in the film state.

Experimental Section

Materials and Instrumentation. Poly[(2,5-dialkoxy-1,4-phenylenevinylene)-*alt*-(1,3-phenylenevinylene)] **4** and **6** were prepared as reported previously.[6a,9] An attempt to convert **6b** to **4b** via refluxing its toluene solution under an argon atmosphere in the presence of 0.3, 0.6, and 0.9 wt % iodine, however, was not successful, as monitored by the film PL spectra. Iodine analysis was performed by Galbraith Laboratories, Inc. The contents of *trans*-CH=CH in the samples were estimated from ^{1}H NMR on a Bruker ARX400 spectrometer. The solutions were prepared by dissolving the samples in freshly distilled dry THF solvent in a quartz NMR tube and deoxygenated by bubbling a slow stream of argon through the solution. UV−vis spectra were recorded on a Hewlett-Packard 8453 diode array spectrophotometer. Fluorescence spectra were recorded on a PTI steady-state fluorometer. A low-temperature sample holder with a Dewar vessel was used for the measurement of the low-temperature spectra. In a typical experiment, liquid nitrogen was used to cool the sample solution. The temperature of −108 °C was conveniently determined by observing the THF solid−solution equilibrium (mp of THF solvent is −108 °C). The films were coated on the surface of a quartz tube of 5 mm diameter and dried under vacuum (<0.2 mmHg). The polymer-coated quartz tube was directly inserted in the low-temperature sample holder for the solid-state spectra at room and low temperature.

LED Device Fabrication and Measurement. PEDOT/PSS (Bayer Co.) was spin-cast onto ITO glass (OFC Co.) to be used as an anode. The polymer solutions (20 mg/mL in chloroform) were filtered through 0.2 μm Millex-FGS filters (Millipore Co.) and were spin-cast onto ITO glass or dried PEDOT/ITO substrates under a nitrogen atmosphere. The polymer films were typically 75 nm thick. Calcium electrodes of 400 nm thickness were evaporated onto the polymer films at about 10^{-7} Torr, followed by a protective coating of aluminum. The devices were characterized using a system constructed in our laboratory described elsewhere.[17]

Conclusions

A systematic study has been carried out to investigate the influence of the iodine-catalyzed isomerization on the optical properties of PmPVpPV. Although little effect is observed in solution, the potential contamination from the iodine-catalyzed isomerization exhibits a noticeable influence on the optical properties of the polymer films, especially at the low temperature. With the aid of the low-temperature spectroscopic study, the majority of emissions from the films are likely originating from the 0−1 and 0−2 transitions. Electroluminescent characteristics show that the iodine contamination may cause imbalanced electron and hole injection, thereby lowering the device efficiency. The iodine-free polymer permits a balanced injection of electron and hole, thus greatly improving the EL efficiency to 0.16% in a device configuration of ITO/PEDOT/polymer/Ca.

Acknowledgment. Support of this work has been provided by AFOSR (Grant F49620-00-1-0090) and by NIH/NIGMS/MBRS/SCORE (Grant S06GM08247).

References and Notes

(1) Burroughes, J. H.; Bradley, D. D. C.; Brown, A. R.; Marks, R. N.; Mackay, K.; Friend, R. H.; Burn, P. L.; Holmes, A. B. *Nature (London)* **1990**, *347*, 539−541.

(2) For a recent review on electroluminescent conjugated polymers, see: Kraft, A.; Grimsdale, A. C.; Holmes, A. B. *Angew. Chem., Int. Ed. Engl.* **1998**, *37*, 402−428.

(3) McGehee, M. D.; Heeger, A. J. *Adv. Mater.* **2000**, *12*, 1655−1668.

(4) McQuade, D. T.; Pullen, A. E.; Swager, T. M. *Chem. Rev.* **2000**, *100*, 2537−2574.

(5) Skotheim, T. A., Elsenbaumer, R. A., Reynolds, J. R., Eds. *Handbook of Conducting Polymers;* Marcel Dekker: New York, 1998.

(6) (a) Pang, Y.; Li, J.; Hu, B.; Karasz, F. E. *Macromolecules* **1999**, *32*, 3946−3950. (b) Davey, A. P.; Drury, A.; Maier, S.; Byrne, H. J.; Blau, W. J. *Synth. Met.* **1999**, *103*, 2478−2479. (c) Ohnishi, T.; Doi, S.; Tsuchida, Y.; Noguchi, T.

Photonic and Optoelectronic Polymers; American Chemical Society: Washington, DC, 1997; pp 345−357.

(7) Guilbault, G. G. *Practical Fluorescence*, 2nd ed.; Marcel Dekker: New York, 1990; Chapter 3.

(8) Ideses, R.; Shani, A. *J. Am. Oil Chem. Soc.* **1989**, *66* (7), 948−952.

(9) Liao, L.; Pang, Y.; Ding, L.; Karasz, F. E. *Macromolecules* **2001**, *34*, 6756−6760.

(10) A few recent examples are: (a) Huang, C.; Huang, W.; Guo, J.; Yang, C.-Z.; Kang, E.-T. *Polymer* **2001**, *42*, 3929−3938. (b) Star, A.; Stoddart, J. F.; Steuerman, D.; Diehl, M.; Boukai, A.; Wong, E. W.; Yang, X.; Chung, S.-W.; Choi, H.; Heath, J. R. *Angew. Chem., Int. Ed.* **2001**, *40* (9), 1721−1725.

(11) The repeating unit of **4b** has a formula $C_{28}H_{36}O_2$ (M_w = 404.6), which contains two phenylenevinylene units. The average molar mass of 202.3 for phenylenevinylene in **4b** is, therefore, used in the calculation.

(12) Turro, N. J. *Modern Molecular Photochemistry*; University Science: Mill Valley, CA, 1991; Chapter 4.

(13) Sheridan, A. K.; Lupton, J. M.; Samuel, I. D. W.; Bradley, D. D. C. *Synth. Met.* **2000**, *111−112*, 531−534.

(14) The relative PL quantum efficiencies of films were estimated, as described previously,[15] to be $\phi_s/\phi_r \approx (F_s/F_r)(A_r/A_s)$. Here the values ϕ, F, and A are the quantum efficiency, fluorescence integration area, and absorbance at excitation wavelength for sample (s) or reference (r) films, respectively. The relative quantum efficiency of film **6b** to **4b** was measured to be $\phi_{\mathbf{6b}}/\phi_{\mathbf{4b}} \approx 1.35$ when excited at 436 nm, which is averaged over four independent measurements.

(15) Li, J.; Pang, Y. *Macromolecules* **1998**, *31*, 5740−5745.

(16) Baigent, D. R.; Friend, R. H.; Lee, J. K.; Schrock, R. R. *Synth. Met.* **1995**, *71*, 2171−2172.

(17) Hu, B.; Karasz, F. E. *Chem. Phys.* **1998**, *227*, 263−270.

MA012144J